CHEMISTRY OF MATERIALS
Article

Chem. Mater. **2010,** *22,* 1901–1907 1901
DOI:10.1021/cm903648c

Near-Infrared Absorption of Monodisperse Water-Soluble PbS Colloidal Nanocrystal Clusters

Chunguang Li, Ying Zhao, Feifei Li, Zhan Shi,* and Shouhua Feng

State Key Laboratory of Inorganic Synthesis and Preparative Chemistry, College of Chemistry, Jilin University, 2699 Qianjin Street, Changchun 130012, P. R. China

Received December 3, 2009. Revised Manuscript Received January 17, 2010

Highly monodisperse PbS colloidal nanocrystal clusters with well controllable size and size distribution, high crystallinity and high water solubility have been successfully synthesized through a modified polyol process. Thiourea stock solution was rapidly injected into diethyene glycol solution containing lead precursor at an elevated temperature to produce PbS clusters.The high reaction temperature allows for control over size and size distribution and yields highly crystalline products. The superior water solubility is achieved by using poly(acrylic acid) as the capping agent. The caboxylate groups of which partially bind to the nanocrystal surface and partially extend into the surrounding water. The uncoordinated caboxylate groups also bring high density of charges to the surface of CNCs at the same time. Moreover, the CNCs exhibit visible or near-infrared absorption even though the overall sizes of the particles are larger than the excitation Bohr radius. This is due to the fact that the clusters are composed of primary nanocrystals and the whole cluster shows optical property similar to the tiny primary nanocrystals.

Introduction

Over the past decades, colloidal nanocrystals have been the object of intensive scientific and technological interest.[1] These nanocrystals often exhibit novel optical, electronic, magnetic, and mechanical properties that cannot be obtained in the bulk materials.[2] Among the various nanocrystals, colloidal semiconductor nanocrystals, especially metal chalcogenide nanocrystals, have been the most studied because of their quantum confinement effects and size dependent photoemission characteristics.[3] However, recent advances in this research field appear to be shifting to create size and shape selective secondary structures of colloidal nanocrystals either by self-assembly or through direct solution growth.[4−8] Manipulation of the secondary structures of nanocrystals is desired in order to combine the ability to harness the size-dependent properties of individual nanocrystals with the possibility to tune collective properties due to interactions between the subunits. This research trend has been evidenced by plenty of interesting works published in the past several years.[9−14]

Lead sulfide (PbS) is an important group IV−VI semiconductor with a very small direct band gap of 0.41 eV (in bulk form) and a large excitation Bohr radius of 18 nm,[15] making the quantum-confined effects more notable even for relatively larger particle sizes. It has been widely used in many fields such as Pb^{2+} ion-selective sensors,[16] photography[17] and solar absorbers.[18] Moreover, it has been found that the third-order nonlinear optical response of PbS nanocrystals is expected to be 30 times larger than that of GaAs and 1000 times larger than that of CdSe materials in the limit of strong confinement, so rendering PbS nanocrystals highly desirable for photonic and optical switching device applications.[19,20]

*Corresponding author. E-mail: zshi@mail.jlu.edu.cn.

(1) (a) Fendler, J. H. *Nanoparticles and Nanostructured Films*; Wiley-VCH: Weinheim, Germany, 1998. (b) Weller, H. *Angew. Chem., Int. Ed.* **1993**, *32*, 41. (c) Rogach, A. L.; Talapin, D. V.; Shevchenko, E. V.; Kornowski, A.; Haase, M.; Weller, H. *Adv. Funct. Mater.* **2002**, *12*, 653.
(2) (a) Sun, S.; Murray, C. B.; Weller, D.; Folks, L.; Moser, A. *Science* **2000**, *287*, 1989. (b) Hyeon, T. *Chem. Commun.* **2003**, 927. (c) Jacobs, K.; Zaziski, D.; Scher, E. C.; Herhold, A. B.; Alivisatos, A. P *Science* **2001**, *293*, 1803. (d) Michler, P.; Imamoglu, A.; Mason, M. D.; Carson, P. J.; Strouse, G. F.; Buratto, S. K. *Nature* **2000**, *406*, 968.
(3) (a) Alivisatos, A. P. *Science* **1996**, *271*, 933. (b) Li, X. H.; Li, J. X.; Li, G. D.; Liu, D. P.; Chen, J. S. *Chem.—Eur. J.* **2007**, *13*, 8754. (c) Warner, J. H. *Adv. Mater.* **2008**, *20*, 784.
(4) Yin, Y.; Alivisatos, A. P. *Nature* **2005**, *437*, 664.
(5) Peng, Z. A.; Peng, X. *J. Am. Chem. Soc.* **2002**, *124*, 3343.
(6) Sun, Y.; Xia, Y. *Science* **2002**, *298*, 2176.
(7) Wang, X.; Zhuang, J .; Peng, Q.; Li, Y. D. *Nature* **2005**, *437*, 121.
(8) Pileni, M. P. *Nat. Mater.* **2003**, *2*, 145.
(9) Narayanaswamy, A.; Xu, H.; Pradhan, N.; Peng, X. *Angew. Chem., Int. Ed.* **2006**, *45*, 5361.
(10) Shevchenko, E. V.; Talapin, D. V.; Kotov, N. A.; O'Brien, S.; Murray, C. B. *Nature* **2006**, *439*, 55.
(11) Hu, X. L.; Gong, J. M.; Zhang, L. Z.; Yu, J. C. *Adv. Mater.* **2008**, *20*, 4845.
(12) Lee, J.; Govorov, A. O.; Kotov, N. A. *Angew. Chem., Int. Ed.* **2005**, *44*, 7439.
(13) Halpert, J. E.; Porter, V. J.; Zimmer, J. P.; Bawendi, M. G. *J. Am. Chem. Soc.* **2006**, *128*, 12590.
(14) Li, C. G.; Zhao, Y.; Wang, L.; Li, G. H.; Shi, Z.; Feng, S. H. *Eur. J. Inorg. Chem.* **2010**, *2010*, 217.
(15) Machol, J. L.; Wise, F. W.; Patel, R. C.; Tanner, D. B. *Phys. Rev. B* **1993**, *48*, 2819.
(16) Hirata, H.; Higashiyama, K. *Bull. Chem. Soc. Jpn.* **1971**, *44*, 2420.
(17) Nair, P. K.; Gomezdaza, O.; Nair, M. T. S. *Adv. Mater. Opt. Electron.* **1992**, *1*, 139.
(18) Chaudhuri, T. K.; Chatteries, S. *Proc. Int. Conf. Thermoelectr.* **1992**, *11*, 40.
(19) Hines, M. A.; Scholes, G. D. *Adv. Mater.* **2003**, *15*, 1844.
(20) Sargent, E. H. *Adv. Mater.* **2005**, *17*, 515.

Published on Web 01/28/2010

There have been many synthetic approaches reported for preparing well-defined PbS nanostructures with diverse morphologies including star-shaped, dendritic, closed nanowires, and hollow structures.[21−26] However, most of these reported methods produce 1D or polyhedral nanostructures. Several studies have explored how nanoparticles/polymer composites affect their electrical, optical, magnetic and enhanced mechanical properties.[27−29] More recently, various PbSe nanostructures have been fabricated in solution through oriented attachment of nanocrystal building blocks.[30,31] For example, Murray[31] and co-workers fabricated nanowires and nanorings through self-assembly of PbSe nanocrystals. However, the assembly of PbS colloidal nanocrystals in a facile manner into advanced secondary structures with continuous size tuning still remains a significant challenge. In this paper, we demonstrate that a simple modification to the traditional polyol process can produce highly water-soluble PbS CNCs with uniform and tunable sizes from ∼155 to ∼240 nm. Polyacylic acid (PAA) was used here as the capping agent to render the particles excellent dispersibility in water. The typical clusters exhibit visible or near-infrared absorption (400−800 nm) although the overall sizes of the particles far exceed the excitation Bohr radius. To the best of our knowledge, this is the first report that PbS of such large particle size still has visible or near-infrared absorption. More interestingly, these highly charged PbS CNCs may self-assemble into periodic structures in aqueous solution and strongly diffract light, showing different color under sunlight. These PbS CNCs could be a promising candidate as functional photonic band gap materials.

Experimental Section

Synthesis. Polyacylic acid (PAA) was purchased from Sigma-Aldrich. Pb(II) acetate (99.5%), Thiourea (TU, 99%), Diethylene glycol (DEG, 99.9%) were obtained from Sinopharm Chemical Reagent Co., Ltd. All chemicals were used as received without further purification.

PbS Colloidal Nanocrystal Clusters. The PbS CNCs were synthesized by means of high-temperature polyol-mediated reaction. TU/DEG stock solution was first prepared by dissolving TU (8 mmol) in DEG (20 mL); this solution was heated at 100 °C for 1 h under nitrogen atmosphere, and kept at room temperature. In a typical synthesis, Pb(II) acetate (0.4 mmol), DEG (6 mL) and PAA (6 mmol) were mixed together, and the mixture was heated to 215 °C under a protective nitrogen atmosphere. TU/DEG (2.0 mL) stock solution was injected rapidly into the hot mixture, and the temperature dropped to about 200 °C instantly. The reaction solution turned black within 1 min and then was further heated 11 min at 210 °C. The products were cooled to room temperature to yield about 155 nm PbS CNCs. The amount of TU/DEG solution determines the size of CNCs. For instance, amounts of stock solution of 1.0−1.2, 1.2−1.5, 1.5−2.0 mL leads to CNCs with average sizes of 240, 180, and 155 nm, respectively. The final product was cleaned three times by precipitation with ethanol followed by centrifugation at 11 000 rpm and finally dispersed in distilled water.

Table 1. Experimental Details for Different PbS CNCs

PbS size (nm)	PAA (mmol)	S/Pb[a]	T (°C)	reaction time	color
155	6	2.0	210	11 min	yellow-green
180	6	1.5	210	11 min	red
240	6	1.0	210	11 min	dark green
27	6	1.0	235	5 s	black

[a] Mole ratio of thiourea to $Pb(Ac)_2$. The concentration of $Pb(Ac)_2$ in 8 mL of DEG was fixed at 0.5 mol/L, whereas different volumes of thiourea/ diethylene glycol (DEG, 4 mol/L) were injected according to the ratio listed in the table.

PbS Nanocubes. The PbS nanocubes were prepared by a similar procedure. Pb(II) acetate (0.4 mmol), DEG (6 mL) and PAA (6 mmol) were mixed together, and the mixture was heated to 235 °C under a N_2 atmosphere. The temperature of the reaction system was blowed to room temperature instantly after injecting TU/DEG stock solution.

Characterazation. Powder X-ray diffraction (XRD) analysis was performed on a Rigaku D/max-2500 diffractometer with a graphite monochromator by using CuKα radiation operating at 200 mA and 40 kV. XRD data were collected over the range of 10−60° (2θ) with a step interval of 0.02° and a preset time of 1.6 s per step at room temperature.Transmission electron microscopy (TEM), high-resolution transmission eletron microscopic (HRTEM) images and EDX spectra were performed on a JEM-2100F electron microscope equipped with an X-ray energy-dispersive spectroscopy system. The IR spectra were acquired on a Bruker IFS 66v/S FTIR spectrometer, whereas Ramam spectra were measured with a Renishaw 2000 model confocal microscopy Raman spectrometer with a CCD detector and a holographic notch filter (Renishaw Ltd., Gloucestershire, U.K.). Radiation of 514.5 nm was given by an air-cooled argon ion laser. All of the Raman spectra were recorded in 10.0 s.

Results and Discussion

Formation, Structure, and Morphology of the CNCs. XRD. PbS CNCs with particle sizes ranging from 155 to 240 nm and PbS nanocubes have been obtained under controlled experimental conditions. Details of these conditions are summarized in Table 1. The phase structures of the as-synthesized PbS CNCs were investigated by XRD. Figure 1 shows the XRD patterns of PbS CNCs with different particle sizes and the standard data for PbS as well. The results of the XRD indicate that these three samples crystallized well, and the patterns are in good agreement with the bulk PbS crystal phase (JCPDS 05−0592). The five major peaks can be indexed as 111,

(21) Wang, Y. L.; Cai, L.; Xia, Y. N. *Adv. Mater*. **2005**, *17*, 473.
(22) Wang, S. F.; Gu, F.; Lv, M. K. *Langmuir* **2006**, *22*, 398.
(23) Zhao, N. N.; Qi, L. M. *Adv. Mater*. **2006**, *18*, 359.
(24) Zhou, G. J.; Lv, M. K.; Xiu, Z. L.; Wang, S. F.; Zhang, H. P.; Zhou, Y. Y.; Wang, S. M. *J. Phys. Chem. B* **2006**, *110*, 6543.
(25) Lee, S.; Jun, Y.; Cho, S.; Cheon, J. *J. Am. Chem. Soc*. **2002**, *124*, 11244.
(26) Peng, Z. P.; Jiang, Y. S.; Song, Y. H.; Wang, C.; Zhang, H. J. *Chem. Mater*. **2008**, *20*, 3153.
(27) Lü, C. L.; Guan, C.; Liu, Y. F.; Cheng, Y. R.; Yang, B. *Chem. Mater*. **2005**, *17*, 2448.
(28) Warner, J. H.; Watt, A. A. R.; Tilley, R. D. *Nanotechnology* **2005**, *16*, 2381.
(29) Babu, K. S.; Vijayan, C.; Haridoss, P. *Materials Science and Engineering C* **2007**, *27*, 922.
(30) Sashchiuk, A.; Amirav, L.; Bashouti, M.; Krueger, M.; Sivan, U.; Lifshitz, E. *Nano Lett*. **2004**, *4*, 159.
(31) Cho, K. S.; Talapin, D. V.; Gaschler, W.; Murray, C. B. *J. Am. Chem. Soc*. **2005**, *127*, 7140.

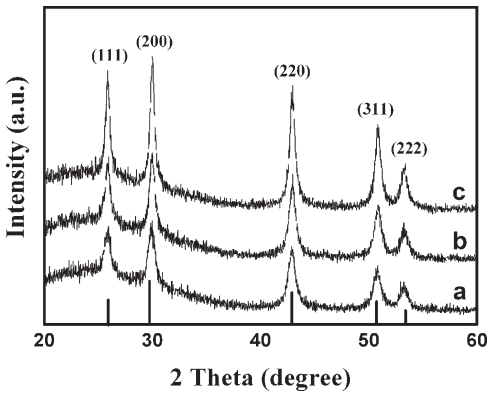

Figure 1. XRD pattern of (a) 155, (b) 185, and (c) 240 nm PbS CNCs. Literature values for the peak positions and intensities for bulk cubic PbS samples are indicated by the vertical bars.

200, 220, 311, 222, respectively. No peaks of other impurities were detected.

TEM and SEM. The polyol process was initially focused on the preparation of monodispersed metals and alloys more than 20 years ago. Later, it has been extensively used for the synthesis of nanoscale oxide, sulfide, phosphate and rare earth materials.[32] The polyol, such as diethylene glycol (DEG), is a good solvent, and can easily dissolve a variety of polar inorganic materials owing to its high permittivity (ε = 32) and boiling points. On the other hand, it shows reducing properties at high temperature. The modified polyol process is described here for the preparation of PbS nanocubes and CNCs. Instead of using the traditional Polyvinylpyrrolidone (PVP) as surfactant, we chose PAA to produce highly water-soluble PbS CNCs. The carboxylate groups of PAA show strong coordination power with Pb^{2+} on PbS surface and the uncoordinated carboxylate groups extend into aqueous solution. Upon introduction of thiourea (TU) into the mixture of DEG, $Pb(Ac)_2$, and PAA at ~215 °C, the very fast decomposition of TU leads to the formation of plenty of S^{2-} in the system. Both nucleation and growth are involved in this procedure and finally PbS nanocrystals are formed. Under optimized conditions, these PbS nanocrystals spontaneously aggregate to form flowerlike three-dimensional clusters, as shown in the representative transmission electron microscopy (TEM) images in Figure 2. The size of the CNCs can be tuned from about 155 to about 240 nm by simply changing the molar ratio of thiourea to $Pb(Ac)_2$ while keeping all the other parameters fixed (Figure 2). This size tunability may be the result of more PbS nuclei caused by higher TU concentration in the reaction mixture, which promote the formation of smaller clusters. The growth of CNCs may follow the well-documented two-stage growth model whereby PbS nanocrystals first nucleate in a supersaturated solution and then aggregate into larger raspberry-like assemblies (~155−240 nm) in

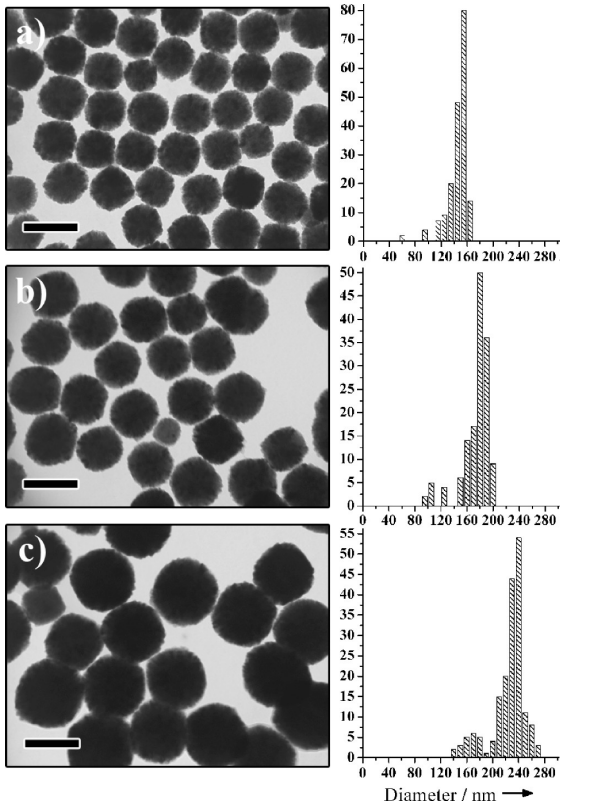

Figure 2. Representative TEM images of PbS CNCs at the same magnification. The average diameters of the CNCs obtained by measuring about 150 clusters for each sample: (a)155, (b)180, and (c) 240 nm. All scale bars are 200 nm.

diameter.[33] The rough surface of both TEM and SEM images (Figure 3) confirms that these monodisperse colloids consist of small primary particles. PbS nanocubes were also obtained at higher temperature and with shorter reaction time to stop the growth of PbS at the first stage (Figure S1 in the Supporting Information).

High-magnification TEM and high-resolution TEM (HRTEM) images provide further insight into the structural information on the secondary structure of PbS CNCs. Figure 4a shows a typical TEM image of an individual cluster of 150 nm in diameter at a high magnification. Clearly, the cluster is composed of small primary crystals with size of 6−8 nm. Its corresponding Fast Fourier Transform (FFT) pattern reveals the single-crystal-like diffraction (Figure 4b). The diffraction spots are widened into ellipses indicating slight misalignments among the primary nanocrystals. Lattice fringes were recorded in the HRTEM image (Figure 4c). The particles are cubic in shape and the FFT pattern of the selected-area in Figure 3c proves that the particle has a single crystalline feature (Figure 4d). This observation demonstrates that the primary nanocrystals are single-crystalline, whereas the whole cluster is polycrystalline. Meanwhile, energy dispersive X-ray (EDX) analysis further confirms the local element composition of the PbS CNCs (Figure S2 in the Supporting Information).

XPS. The above analyses, such as X-ray diffraction, TEM, and FFT pattern, clearly show the formation of PbS nanoparticles. A chemical analysis of the sample was

(32) (a) Feldmann, C. *Adv. Mater.* **2001**, *13*, 1301. (b) Feldmann, C. *Adv. Funct. Mater.* **2003**, *13*, 101. (c) Feldmann, C.; Jungk, H. O. *Angew. Chem., Int. Ed.* **2001**, *40*, 359. (d) Feldmann, C.; Metzmacher, C. *J. Mater. Chem.* **2001**, *11*, 2603. (e) Zheng, Q. L.; Zhang, Y. *Angew. Chem., Int. Ed.* **2006**, *45*, 7732.

(33) Libert, S.; Gorshkov, V.; Goia, D.; Matijevi, E.; Privman, V. *Langmuir* **2003**, *19*, 10679.

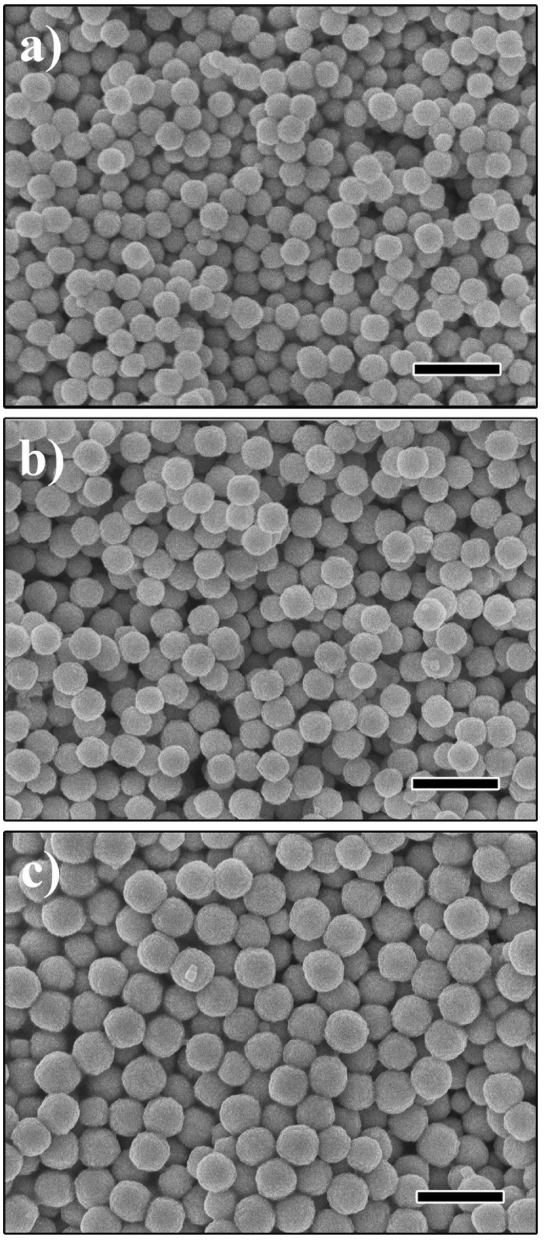

Figure 3. SEM images of PbS CNCs with different particle sizes of (a) 155, (b) 180, and (c) 240 nm. All scale bars are 500 nm.

also carried out using X-ray photoelectron spectroscopy to substantiate these data. The photoelectron spectroscopy of the sample over a wide range of binding energies is shown in Figure 5a. It is very clear that Pb, S, C, and O are the only prominent elements present in the sample. Detailed spectra of the Pb 4f and S 2p core levels are shown in panels b and c in Figure 5, respectively. Pb $4f_{7/2}$ at 137.7 eV and S $2p_{3/2}$ at 161.9 eV are in good agreement with the core level binding energies tabulated earlier.[34] As seen in Figure 5c, the peak of S 2p core level is quite broad, probably due to the contributions from the sulfur in PbS and the associated polymer capping agent. These analyses show that pure PbS nanoparticles indeed existed. However,because of the existence of polymer capping agent on

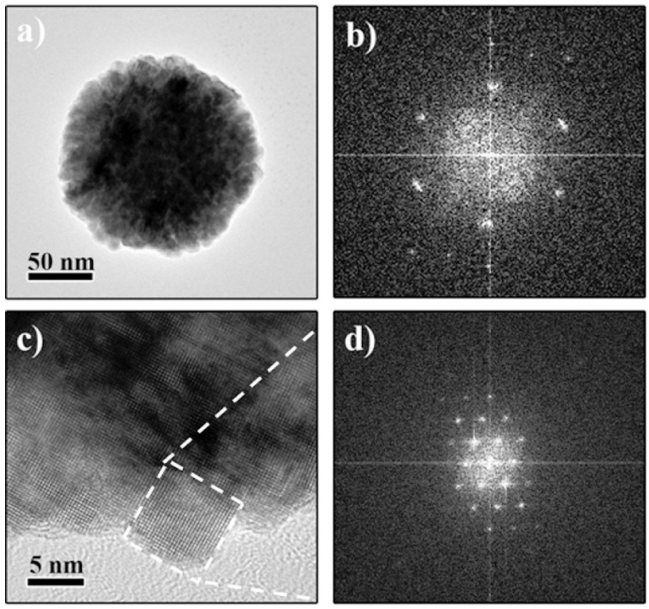

Figure 4. (a) High-magnification TEM image of a 155-nm CNCs. (b) FFT of the PbS colloidal nanocrystal cluster shown in a. (c) Typical HRTEM image of a 180 nm cluster. (d) FFT patterns obtained by using program Image-Pro Plus 5.0 of the corresponding areas in c.

the surface of PbS CNCs, they are initially associated with elements such as carbon and oxygen. O1s and C1s appear at 531.1 and 285 eV, respectively (Figure 5a).

FTIR. A very important improvement in our synthesis is to use PAA to replace the widely used PVP as the surfactant. The coordination of carboxylate to PbS surface is very strong and the uncoordinated carboxylate groups on the polymer chains render the products excellent water solubility. The stability of PAA on PbS surface was demonstrated by measuring the Fourier Transform Infrared Spectroscopy (FTIR) spectrum on a sample that was repeatedly washed and then dried to powder. The multiple bands between 1200 and 1600 cm^{-1} shown in Figure 6a can be assigned to various vibrational modes of PAA, and the strong adsorption band at around 1717 cm^{-1} is characteristic of the C=O stretching mode for protonated carboxylate group. For comparison, in Figure 6b, the three peaks located at 1455, 1586, and 1415 cm^{-1} can be attributed to the characteristic bands of the carboxylate (COO^-) groups, corresponding to the CH_2 bending mode and asymmetric and symmetric C−O stretching modes of the COO^- group, respectively.[35,36] A comparison of these two spectra shows clearly that many carboxylate groups remain on the surface of nanocrystals even after excessive washing. The uncoordinated carboxylate groups on the polymer chains can also be protonated by adding HCl to adjust the pH value below to 4, at which the particles start to aggregate and precipitate out from the solution. The FTIR spectrum of such a precipitate is shown in Figure 6c. The strong peak around 1717 cm^{-1} similar to PAA appears due to the C=O stretching mode for protonated carboxylate groups. This result indicates that the high solubility of

(34) Chastain, J. *Handbook of X-ray Photoelectron Spectroscopy*; Perkin-Elmer, Norwalk, CT, 1992.
(35) Lee, D. H.; Condrate, R. A.; Reed, J. S. *J. Mater. Sci.* **1996**, *31*, 471.
(36) Li, H.; Tripp, C. P. *Langmuir* **2005**, *21*, 2585.

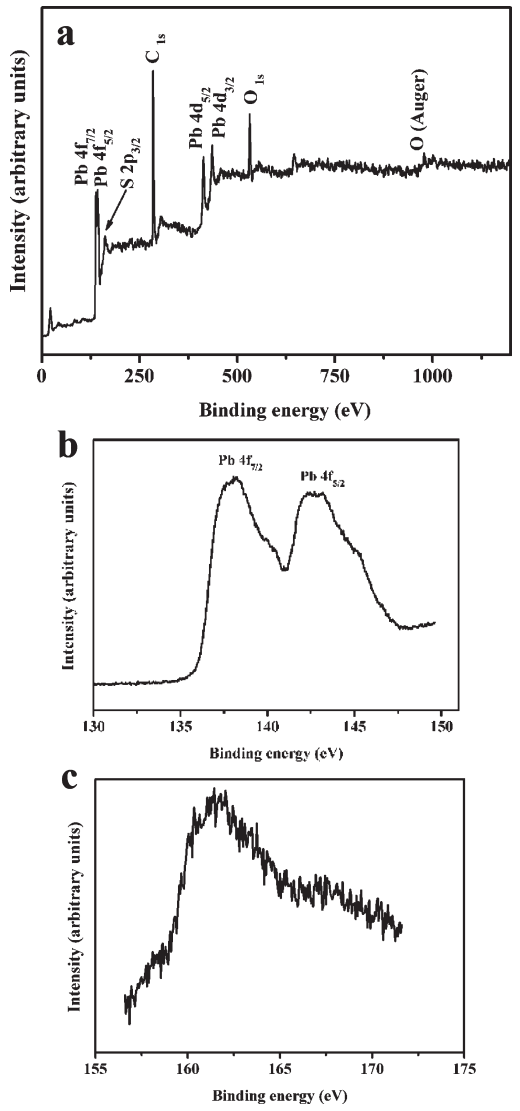

Figure 5. X-ray photoelectron spectra of PbS CNCs: (a) survey scan, (b) Pb 4f core level, (c) S 2p core level.

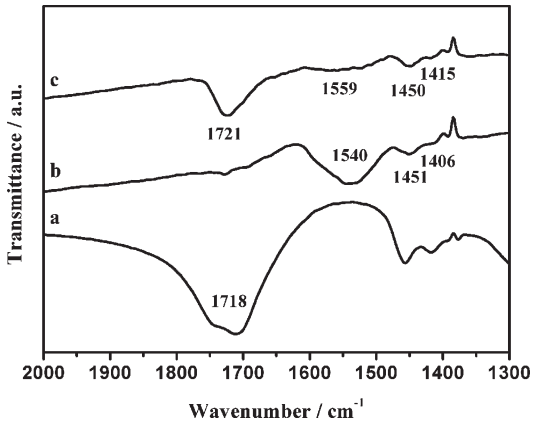

Figure 6. FTIR spectrum of (a) pure PAA, (b) carboxylate-capped PbS CNCs, and (c) carboxyl-capped PbS CNCs.

the particles is due to the carboxylate groups ionized at higher pH. In the weak acid solution, the surface carboxylate groups are partially protonated so that the solubility of the particles decreases. We have also tested the stability

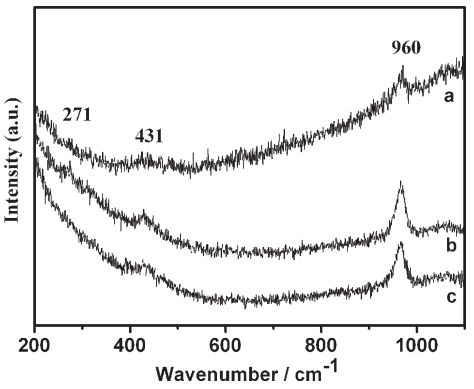

Figure 7. Raman spectrum of carboxylate-capped PbS CNCs: (a) 155, (b) 180, and (c) 240 nm.

of the PbS colloids in water through measuring their diameters at various time intervals. As shown in Figure S3 in the Supporting Information, the particle size exhibits nearly no change after 10 test cycles, indicating that the PbS colloids could stably disperse in water for long time, especially the PbS nanocubes which can disperse in water for half a year without precipitation.

Raman. We used Raman spectrum to characterize the structure information of as-prepared CNCs (Figure 7). Because of its high adsorption under 514.5 nm excitation, PbS is a relatively weak Raman scatter at room temperature and susceptible to laser-induced degradation upon intense irradiation.[38] Furthermore, some parameters such as particle size, temperature, excitation wavelength, and crystallographic facet have a great effect on the peak wavenumber and intensity. Here, relatively higher power (25 mW) is applied to irradiate the CNCs in order to investigate their stabilities toward laser irradiation rather than the Raman spectrum of PbS itself. Under irradiation, peaks centered around 270, 341, and 960 cm^{-1} are clearly observed for the samples. These peaks could be attributed to the formation of lead oxysulfate and oxide such as $PbO \cdot PbSO_4$, $PbO \cdot 4PbSO_4$, and PbO as photooxidation products of PbS.[37,38] Different peaks with varied intensity from photooxidant products of PbS CNCs can be observed. Analogous analysis reveals that 180 and 240 nm PbS CNCs located in the intermediated position are similar in terms of irradiation stability. An exception is the PbS CNCs of 155 nm with near absence of any peaks except the weak peak at ~960 cm^{-1}, which suggests that it is the most stable one among the three kinds of clusters.

Optical Properties. The absorption spectra of the as-synthesized PbS CNCs and nanocubes are shown in Figure 8. Compared with bulk PbS, which has an absorption onset at about 3020 nm, the absorption edge of PbS nanostructures obtained by us exhibits a large blue-shift. The particle size of 27,155, 180, and 240 nm leads to the corresponding absorption peak of 278, 436, 644, and 818 nm, respectively. This result is fantastic because the

(37) Smith, G. D.; Firth, S.; Clark, R. J. H.; Cardona, M. *J. Appl. Phys.* **2002**, *92*, 4375.
(38) Batonneau, Y.; Bremard, C.; Laureyns, J.; Merlin, J. C. *J. Raman Spectrosc.* **2000**, *31*, 1113.

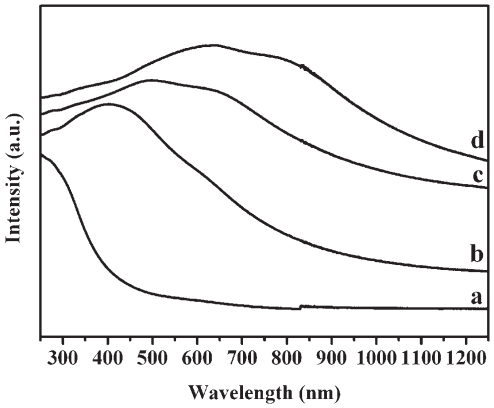

Figure 8. Absorption spectra of a size series of PbS nanocrystals: (a) nanocubes and (b)155, (c) 180, and (d) 240 nm cluster.

overall sizes of the particles are larger than the Bohr radius. To PbS nanocubes, it may be because of the existence of position-dependent quantum-size effects, which was speculated by Qi and co-workers for the relatively large but highly faceted nanocrystals with regular shapes, and which results in dramatically blue-shifted excitonic absorptions.[39a] Another possibility is that the observed peaks may correspond to transitions into high-energy bands rather than excitonic transitions.[39] The particle size of PbS CNCs ranging from about 155 nm to about 240 nm far exceeds the excitation Bohr radius, but they still show visible and near-infrared absorption(Figure 8b−d). Calculations with the Debye−Scherrer formula for the strongest peak (200) gave grain sizes of 13.5, 14.7, and 16.7 nm for CNCs with sizes of 155, 180, and 240 nm, respectively; this implies that the primary nanocrystals grow slightly with the increasing size of CNCs. This result indicates that the size of primary nanocrystals increases with lower molar ratio of Pb:S, which means that small size clusters have smaller primary nanocrystals at the same time. The different size of primary nanocrystals leads to red shift of the optical absorption edge from 436 to 818 nm of the absorption spectra. TEM and HRTEM images of these three samples also agree well with the trends of XRD data as shown in Figure S4 in the Supporting Information. Therefore, both XRD data and TEM images clearly show that the smaller size of primary nanocrystals corresponds to shorter wavelength of absorption spectra. Because the optical properties of the clusters are almost certainly related to the size of the primary nanocrystals, we could obtain PbS CNCs with different size of primary nanocrystals through controlling over the reaction conditions such as the concentration of initial metal precursors, temperature, and reaction time to conveniently tune their optical property.

Highly charged monodisperse colloidal particles spontaneously self-assemble into face-centered cubic or body-centered cubic crystalline colloidal arrays in low ionic strength aqueous solutions. They are the simplest

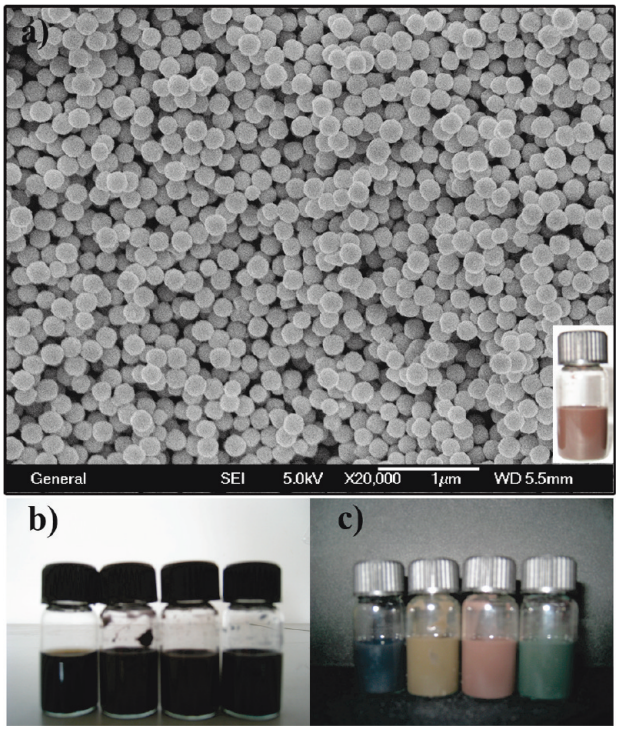

Figure 9. (a) SEM image of polyacrylate-capped PbS colloidal nanocrystals clusters. Inset: corresponding photograph of red color CNCs. (b) Photograph of PbS CNCs directly dispersed in the water without light illuminating. (c) Photograph of colloidal crystals formed in response to light illuminating; the particle size increases gradually from left to right.

photonic crystals showing bandgaps only in particular directions.[40−45] Polyacylic acid capping on the surface of PbS colloidal nanocrystal clusters confers upon the particles not only a high degree of dispersibility but also many charges around the surface of CNCs. The high-density charges of colloid surface leads to the existence of strong repulsive electrostatic interactions between these PbS colloids. The repulsive force could partially balance the gravitation of PbS itself so that the large size of CNCs can still disperse in aqueous solution for several days. The combination of relatively large particle size, high particle uniformity and highly charged surface make these PbS CNCs the ideal building block for the fabrication of light responsive photonic crystals. From Figure 9a, it can be seen that uniform PbS CNCs of 180 ± 5 nm are produced through the modified polyol process without any size-sorting process. More interestingly, these PbS CNCs strongly diffract light and show red color under sunlight. Other PbS CNCs with different diameters and PbS nanocubes are also prepared by a similar procedure (Figure 9b). Considering that these simplest photonic crystals show bandgaps only in particular directions, very dark blue dispersion is observed in water when the direction of sunlight irradiation is blocked, whereas various colors can be observed under irradiation even

(39) (a) Zhao, N. N.; Qi, L. M. *Adv. Mater.* **2006**, *18*, 359. (b) Dong, L. H.; Chu, Y.; Zhuo, Y. J.; Zhang, W. *Nanotechnology* **2009**, *20*, 125301.
(40) Rundquist, P. A.; Photinos, P.; Jagannathan, S.; Asher, S. A. *J. Chem. Phys.* **1989**, *91*, 4932.
(41) Pradhan, R. D.; Bloodgood, J. A.; Watson, G. H. *Phys. Rev. B* **1997**, *55*, 9503.
(42) Ge, J.; Hu, Y.; Yin, Y. *Angew. Chem., Int. Ed.* **2007**, *46*, 7428.
(43) Krieger, I. M.; O'Neill, F. M. *J. Am. Chem. Soc.* **1968**, *90*, 3114.
(44) Hiltner, P. A.; Krieger, I. M. *J. Phys. Chem.* **1969**, *73*, 2386.
(45) Xu, X. L.; Friedman, G.; Humfeld, K. D.; Majetich, S. A.; Asher, S. A. *Chem. Mater.* **2002**, *14*, 1249.

when other directions become dark (Figure 9c). The different colors of these PbS CNCs are related to the particle size. As shown in Figure 9c, as the diameter of CNCs increases gradually from left to right, the color turns black, green-yellow, red and dark green, respectively. A comparison among the photos of PbS in Figure 9 indicates that the very uniform and highly charged PbS CNCs form periodic structures with regular interparticle spacing of a few hundred nanometers according to the different particle size so that the system strongly diffracts light.

Conclusions

In summary, a modified polyol process has been developed to synthesize monodisperse PbS colloidal nanocrystal clusters which are composed of small primary nanocrystals. The cluster size can be tuned from about 155−240 nm through varying the molar ratio of Pb^{2+} to thiourea. PbS nanocubes are also successfully synthesized at higher reaction temperature. Surface-tethered PAA polymer chains render the particles highly water-dispersible. The uncoordinated carboxylate groups extend to the aqueous solution, rendering the clusters high surface charges, and thus producing efficient repulsive force between colloids. These clusters spontaneously self-assemble into periodic structures with regular interparticle spacing and strongly diffract light only in particular directions. The very uniform and highly charged monodisperse PbS clusters could serve as an ideal building block for the fabrication of light responsive photonic crystals. More importantly, the three typical clusters exhibit visible or near-infrared absorption (400−800 nm) even though the overall sizes of the particles far exceed the excitation Bohr radius, which is a very important feature and difficult to achieve though other synthetic methodologies.

Acknowledgment. This work was supported by the Foundation of the National Natural Science Foundation of China (20671040, 20971054, and 90922034), New Century Excellent Talents in University, and the Key Project of Chinese Ministry of Education.

Supporting Information Available: TEM image and size distribution of PbS nanocubes; EDX spectrum of a single PbS CNC; particle diameter during ten test cycles; typical HRTEM images of three kinds of PbS CNCs samples (PDF). This material is available free of charge via the Internet at http://pubs.acs.org.